

# Structural characterization, genotoxicity and electrochemical properties of the Schiff base ligands and their Ni(II) complexes\*

C. ÇELİK<sup>\*</sup>, M. ASLANTAŞ<sup>a</sup>, E. ŞAHİN<sup>b</sup>, A. KAYRALDIZ<sup>c</sup>, M. TÜMER

*Chemistry Department, Kahramanmaraş Sutcuimam University, 46100 Kahramanmaraş, Turkey*

*<sup>a</sup> Physics Department, Kahramanmaraş Sutcuimam University, 46100 Kahramanmaraş, Turkey*

*<sup>b</sup> Chemistry Department, Ataturk University, 25100 Erzurum, Turkey*

*<sup>c</sup> Biology Department, Kahramanmaraş Sutcuimam University, 46100 Kahramanmaraş, Turkey*

Schiff base ligands ( $H_2L^1$  and  $H_2L^2$ ) and their metal complexes were prepared and characterized by analytical and spectroscopic methods. The electrochemical properties of the ligands and complexes were investigated in different solvents. The structure, ( $H_2L^1$ ), of  $C_{20}H_{22}N_2O_2$  was determined by X-ray crystallography. It crystallizes in a monoclinic system, space group C2, with lattice parameters  $a = 15.983(4)$ ,  $b = 11.845(2)$ ,  $c = 9.646(2)$  Å,  $\beta = 98.500(16)^\circ$ ;  $V = 1806.0(7)$  Å<sup>3</sup> and  $Z = 4$ . The ligands were mutagenic on the *S. Typhimurium TA98* strain in the presence and/or absence of a S9 mix. The ligands showed mutagenic activity on the strain TA 100, with and without a S9 mix.

(Received November 5, 2008; accepted December 15, 2008)

*Keywords:* Schiff base ligands, genotoxicity, cyclic voltammetry, X-ray structure

## 1. Introduction

Schiff bases (SB), so called since their synthesis was first reported by Schiff [1], result from the condensation of primary amines with aldehydes and ketones, and contain a C=N double bond. This direct reaction is the most common method for obtaining a SB. Other synthetic methods have been widely reviewed by Dayagi and Degani [2]. However, few SBs commonly used as ligands have been prepared and characterized in their uncomplexed state, since the corresponding metal complexes were directly obtained by other procedures [3]. Thus, many metal complexes containing  $H_2$  salen may be obtained directly by reaction between metal ions, salicylaldehydes and ethylenediamine [4].

In this study, we prepared two racemic Schiff base ligands and their nickel(II) complexes. The X-ray structure of the Schiff base ligand  $H_2L^1$  was performed. The genotoxicity and electrochemical properties of the ligands in the DMSO, DMF and  $CH_3CN$  solutions were studied.

## 2. Experimental

### 2.1 General

All organic and inorganic substances were obtained from Fluka. Elemental analyses (C, H, N) were performed using a LECO CHNS 932 elemental analyser. I.r. spectra were obtained using KBr discs ( $4000-400\text{ cm}^{-1}$ ) on a Shimadzu 8300 FT-IR spectrophotometer. The electronic spectra in the 200-900 nm range were obtained on a Shimadzu UV-160 A spectrophotometer. The mass spectra of the ligands were recorded on a LC/MS APCI AGILENT 1100 MSD spectrophotometer (TUBITAK). <sup>1</sup>H and <sup>13</sup>C n.m.r. spectra were recorded on a Varian XL-200 instrument. TMS was used as an internal standard and deuterated methanol as a solvent. Cyclic voltammograms were recorded on an Iviumstat Electrochemical workstation equipped with a low current module (BAS PA-1) recorder. The electrochemical cell was equipped with a BAS glassy carbon working electrode (area 4.6 mm<sup>2</sup>), a platinum coil auxiliary electrode and a Ag/AgCl reference electrode filled with tetrabutylammonium tetrafluoroborat ( $[CH_3(CH_2)_3]_4NBF_4$ ), 0.1 M in DMSO, DMF and  $CH_3CN$ , Aldrich) solution and adjusted to 0.00 V vs. SCE.

\* Paper presented at the International School on Condensed Matter Physics, Varna, Bulgaria, September 2008

## 2.2 Preparation of the ligands ( $H_2L^1$ and $H_2L^2$ )

The ligands were prepared according to the literature [5].  $H_2L^1$ : Yield: 85 %, color: yellow, M.p.: 113 °C. Elemental analyses, found (calcd. %): C, 74.54 (74.51); H, 6.86 (6.88); N, 8.71 (8.69).  $^1H$  NMR: ( $CD_3OD$  as solvent,  $\delta$  in ppm):  $\delta$  10.15 (s, OH, 2H), 8.34 (s, CH=N, 2H), 6.72–7.28 (m, Ar–H, 8H), 3.41–1.19 (m, CH/CH<sub>2</sub>, 10H);  $^{13}C$  NMR: ( $CD_3OD$  as solvent,  $\delta$  in ppm):  $\delta$  168.41 (CH=N), 119.63–135.37 (Ar–C), 52.08–27.08 (CH/CH<sub>2</sub>). Mass Spectrum (LC/MS APCI): m/z 323 [ $M$ ]<sup>+</sup> (30 %), 324 [ $M+1$ ] (27 %), 325 [ $M+2$ ]<sup>+</sup> (20 %), 110 [ $C_6H_{10}N_2$ ]<sup>+</sup> (100 %). UV-Vis: ( $\lambda_{max}$ , nm,  $\epsilon_{max}$  ( $M^{-1}cm^{-1}$ ), EtOH as solvent): 403 (3212), 316 (2418), 274 ( $1.3 \times 10^{-3}$ ). FT-IR: (KBr,  $cm^{-1}$ ): 3420  $\nu(OH)$ , 2934  $\nu(CH_2)$ , 1627  $\nu(CH=N)$ , 1278  $\nu(C-OH)$ .  $H_2L^2$ : Yield: 85 %, color: yellow, M.p.: 145 °C. Elemental analyses, found (calcd. %): C, 69.05 (69.09); H, 6.88 (6.85); N, 7.35 (7.32).  $^1H$  NMR: ( $CD_3OD$  as solvent,  $\delta$  in ppm):  $\delta$  10.82 (s, OH, 2H) 8.33 (s, CH=N, 2H), 6.62–6.95 (m, Ar–H, 6H), 3.81 (s, OCH<sub>3</sub>, 6H), 3.35–1.25 (m, CH/CH<sub>2</sub>, 10H);  $^{13}C$  NMR: ( $CD_3OD$ ):  $\delta$  168.68 (CH=N), 117.62–157.33 (Ar–C), 58.39 (OCH<sub>3</sub>), 52.07–27.00 (CH/CH<sub>2</sub>). MS (LC/MS APCI): m/z 383 [ $M$ ]<sup>+</sup> (17 %), 275 [ $C_{14}H_{14}N_2O_4 + 1$ ]<sup>+</sup> (20 %), 273 [ $C_{14}H_{13}N_2O_4$ ]<sup>+</sup> (100 %). UV-Vis: ( $\lambda_{max}$ , nm,  $\epsilon_{max}$  ( $M^{-1}cm^{-1}$ ), EtOH as solvent): 422 (4269), 323 (5187), 302 (5995), 295 (4269), 276 ( $6.6 \times 10^{-3}$ ). FT-IR: (KBr,  $cm^{-1}$ ): 3452  $\nu(OH)$ , 2936  $\nu(CH_2)$ , 1628  $\nu(CH=N)$ , 1256  $\nu(C-OH)$ .

## 2.3 Preparation of the complexes

The complexes were prepared as in the literature [5].  $NiL^1$ : Yield: 69 %, color: light green, M.p.: > 250 °C. Elemental analyses, found (calcd. %): C, 63.40 (63.37); H, 5.35 (5.32); N, 7.41 (7.39); Ni, 15.54 (15.48).  $^1H$  NMR: ( $CD_3OD$  as solvent,  $\delta$  in ppm):  $\delta$  8.21 (s, CH=N, 2H), 6.43–7.48 (m, Ar–H, 8H), 3.34–1.24 (m, CH/CH<sub>2</sub>, 10H);  $^{13}C$  NMR: ( $CD_3OD$  as solvent,  $\delta$  in ppm):  $\delta$  168.77 (CH=N), 120.02–137.89 (Ar–C), 52.77–25.62 (CH/CH<sub>2</sub>). Mass Spectrum (LC/MS APCI): m/z 379 [ $M$ ]<sup>+</sup> (27 %), 380 [ $M+1$ ] (22 %), 297 [ $C_{14}H_{10}N_2NiO_2$ ]<sup>+</sup> (100 %). UV-Vis: ( $\lambda_{max}$ , nm,  $\epsilon_{max}$  ( $M^{-1}cm^{-1}$ ), EtOH as solvent): 548 (288), 415 (3218), 404 (1269), 316 (5445), 276 ( $7.1 \times 10^{-4}$ ). FT-IR: (KBr,  $cm^{-1}$ ): 2934  $\nu(CH_2)$ , 1615  $\nu(CH=N)$ , 1380  $\nu(C-OH)$ , 510  $\nu(M-O)$ , 445  $\nu(M-N)$ .  $NiL^2$ : Yield: 72 %, color: light green, M.p.: > 250 °C. Elemental analyses, found (calcd. %): C, 60.14 (60.17); H, 5.54 (5.51); N, 6.35 (6.38); Ni, 13.34 (13.37).  $^1H$  NMR: ( $CD_3OD$  as solvent,  $\delta$  in ppm):  $\delta$  8.25 (s, CH=N, 2H), 6.38–7.15 (m, Ar–H, 6H), 3.67 (s, OCH<sub>3</sub>, 6H), 3.22–1.20 (m, CH/CH<sub>2</sub>, 10H);  $^{13}C$  NMR: ( $CD_3OD$  as solvent,  $\delta$  in ppm):  $\delta$  164.21 (CH=N), 115.04–152.15 (Ar–C), 56.52 (OCH<sub>3</sub>), 50.13–26.76

(CH/CH<sub>2</sub>). Mass Spectrum (LC/MS APCI): m/z 439 [ $M$ ]<sup>+</sup> (35 %), 440 [ $M+1$ ] (28 %), 357 [ $C_{16}H_{14}N_2NiO_4$ ]<sup>+</sup> (100 %). UV-Vis: ( $\lambda_{max}$ , nm,  $\epsilon_{max}$  ( $M^{-1}cm^{-1}$ ), EtOH as solvent): 597 (228), 460 (693), 389 (5208), 345 (2935), 275 ( $7.6 \times 10^{-4}$ ). FT-IR: (KBr,  $cm^{-1}$ ): 2936  $\nu(CH_2)$ , 1618  $\nu(CH=N)$ , 1325  $\nu(C-OH)$ , 505  $\nu(M-O)$ , 448  $\nu(M-N)$ .

Table 1. Crystal and experimental data for  $H_2L^1$ .

Empirical formula	$C_{20}H_{22}N_2O_2$
Formula weight	322.40
Temperature	293(2) K
Wavelength	0.71073 Å
Crystal system, space group	Monoclinic, C2
Cell dimensions	a = 15.983(4) Å b = 11.845(2) Å c = 9.646(2) Å $\beta = 98.500(16)^\circ$ 1806.0(7) Å <sup>3</sup>
Cell volume	1806.0(7) Å <sup>3</sup>
Z	4
Density (calculated)	1.186 Mg / m <sup>3</sup>
Absorption coefficient	0.077 mm <sup>-1</sup>
$F_{000}$	688
Crystal size	0.2 x 0.2 x 0.2 mm
$\Theta$ (°) range for data collection	2.58 to 30.56
Index ranges	-22 ≤ h ≤ 22 -16 ≤ k ≤ 16 -13 ≤ l ≤ 12
Reflections collected / unique	26621 / 5256 [R(int) = 0.0625]
Refinement method	Full-matrix least-squares on $F^2$
Data / restraints / parameters	5256 / 2 / 227
Goodness-of-fit on $F^2$	1.046
Final R indices [I > 2σ(I)]	$R_1 = 0.0604$ , $wR_2 = 0.1619$
Extinction coefficient	0.0097(13)
Largest diff. peak and hole	0.137 and -0.167 eÅ <sup>-3</sup>
CCDC deposition number	CCDC-639678

## 2.4 X-ray data collection, structure solution and refinement for the ligand $H_2L^1$

A diffraction experiment for a needle pale yellow crystal of the ligand  $H_2L^1$  was carried out on a four-circle Rigaku R-Axis RAPID-S diffractometer equipped with a two-dimensional area IP detector. Integration of the intensities, correction for Lorentz and polarization effects and cell refinement was performed using CrystalClear software [6]. The structure was solved using SHELXS-97 and refined using a SHELXL-97 [7] software package. All hydrogen atoms were located in geometrically idealized positions (C–H=0.93–0.98 and O–H=0.82 Å) and treated as riding, with  $U_{iso}(H)=1.2U_{eq}(C)$  or  $1.5U_{eq}(O)$ . A summary of the key crystallographic information is given in Table 1.

## 2.5 Ames test

The substances including the medium, the buffers and the S9 mix used in the Ames test were prepared as described in the study of Kayraldiz et al. [8] with chemicals purchased from Sigma, Aldrich, Boehringer Mannheim. Histidin deficient *Salmonella typhimurium* strains, TA98 and TA100 were provided by J.L. Swezey (Microbial Genomics and Bioprocessing Research Unit, North University, Illinois, USA).

### 3. Results and discussion

In this study, we prepared the Schiff base ligands 2- $\{(E)-[[(1S)-2-\{(1E)-(2\text{-hydroxyphenyl)methylene}\}amino]\text{-cyclohexyl}]\text{imino}\}$ methyl}phenol ( $H_2L^1$ ) and 2-methoxy-6- $\{(E)-[[(1S)-2-\{(1E)-(3\text{-methoxy-2-hydroxyphenyl)methylene}\}amino]\text{cyclohexyl}]\text{imino}\}$ methyl}phenol ( $H_2L^2$ ) and their nickel(II) metal complexes. Previously, we reported the X-ray structure of the ligand  $H_2L^2$  [9]. The ligands and complexes are racemic in mixture. All compounds (Fig. 1) were characterized by analytical and spectroscopic methods.

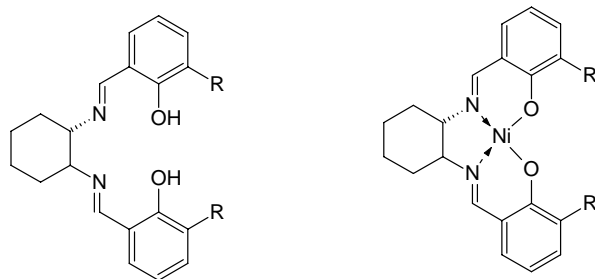


Fig. 1. Proposed structures of the synthesized ligands and their nickel(II) complexes, R: H ( $H_2L^1$ ),  $-OCH_3$  ( $H_2L^2$ ).

In the  $^1H$ -NMR spectra of the ligands, the broad signals at  $\delta$  10.15 and 10.82 ppm may be due to the hydrogen atoms of the hydroxyl groups. In the complexes, these broad bands disappear and this situation confirms that the oxygen atom of the OH group is coordinated to the nickel(II) ion. The azomethine groups are shown at  $\delta$  8.34 and 8.33 ppm as a singlet. In the complexes, these groups shift to the lower regions, and this shows that the nitrogen atom of the  $CH=N$  group is coordinated to the metal ion. Aromatic ring protons are shown in the range  $\delta$  6.62–7.28 ppm range as a multiplet. A signal in the 3.81 ppm region for the ligand  $H_2L^2$  only is due to the presence of the methoxy group. The hydrogen atoms of the  $CH_2/CH$  groups in the cyclohexane ring are observed in the range  $\delta$  3.41–1.19 ppm. Detailed information about the ligands and complexes has been obtained from the  $^{13}C$  NMR spectra. In the ligands, the azomethine carbon atom is shown at  $\delta$  168.41 and 168.68 ppm. In the complexes, this signal shifts to lower regions. The aromatic ring C atoms have been shown in the range  $\delta$  117.62–157.33 ppm. The methoxy carbon atom of the ligand  $H_2L^2$  is shown at 58.39 ppm. The C atoms of the cyclohexane ring are shown in the range  $\delta$  27.00–52.08 ppm. In the spectra of the complexes, the peaks for the carbon atoms shift to lower regions.

The structure of the ligand  $H_2L^1$  has been originally solved by X-ray diffraction [9]. As a result of a structural comparison between the present and previous reported structures, our findings show that the redetermination of the X-ray crystal structure of the compound is imperative

to achieve valuable information on the molecular geometry, conformation, packing and hydrogen-bond geometry, which were not mentioned in the earlier report. Therefore, we report here an X-ray crystal diffraction analysis of the ligand  $H_2L^1$ .

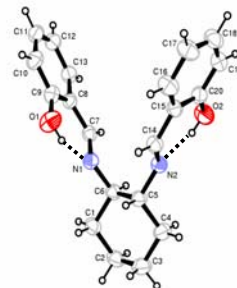


Fig. 2. The molecular structure of the  $H_2L^1$ .

The ORTEP [10] diagram of the molecule, indicating the atom numbering scheme with thermal ellipsoids at 30% probability, is illustrated in Fig.2. The hydrogen bonding geometry is listed in Table 2. In the molecule, the six-membered cyclohexane ring has an ideal chair conformation and all the geometric parameters in the ring are quite normal. Each salicylidene moiety in the molecule is almost planar; the maximum deviations from the mean plane are  $-0.030(3)$  and  $-0.053(2)$  Å for atoms C19 and C7, respectively. All bond lengths and angles in the salicylidene moieties have normal values and are comparable to the literature values [9,11]. The dihedral angle between the planes of the salicylidene moieties [ $56.65(6)^\circ$ ] agrees well with the previous report [9], and is approximately  $6^\circ$  smaller than that ( $62.65(4)^\circ$ ) reported in [11].

Table 2. Hydrogen-bond geometry (Å,  $^\circ$ ) for  $H_2L^1$ .

D-H...A	D-H	H...A	D...A	D-H...A
O1-H9 ... N1	0.82	1.870	2.6017	148
O2-H20 ... N2	0.996	1.870	2.6003	148
C14-H14 ... O1 <sup>i</sup>	0.98	2.921	3.299	105
C10-H10 ... O2 <sup>ii</sup>	0.93	2.678	3.299	124
C11-H11 ... O2 <sup>ii</sup>	0.93	2.680	3.299	124

Symmetry code: (i) x, -y+1, +z+0.5; (ii) x, +y, z-1.

The primary interaction between the molecules in the cell is van der Waals in nature, and a number of O-H...N and C-H...O types of hydrogen bondings are observed in the structure. The O atoms of the hydroxyl groups in the molecule form two strong intra-molecular O-H...N hydrogen bonds ( $H9\cdots N1=1.87$  and  $H20\cdots N2=1.87$  Å), which stabilize the molecule internally. Similar interactions (1.86 and 1.92 Å) were found in [9], and (1.768(18) and 1.783(19) Å) in [11]. In addition, there are intermolecular weak C-H...O interactions which help to stabilize the molecules in the crystal.

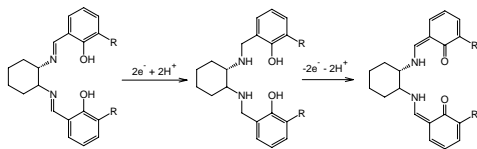


Fig. 3. Reduction-oxidation processes of the Schiff base ligands in the 0.1 M DMSO, DMF and  $CH_3CN$  solutions.

Cyclic voltammogram of the ligand  $H_2L^2$  shows two redox pairs, corresponding to the irreversible two-electron reduction. In the cathodic region, irreversible two-electron reduction may be due to the reduction of the imine group. In other words, the phenolic  $-OH$  groups are oxidized to the keto forms in the anodic potentials as an irreversible process. According to the obtained results, in the same solvents, the ligands exhibit similar irreversible reduction potentials, qualitatively speaking, that the ligands have similar reactivity and similar electrochemical behavior.

Apart from a small change in the oxidation potential, the shape of the waves was unaffected by changing the scan rate. In the same solvents, the obtained data for the ligands are different from each other. The ligand  $H_2L^2$  has the  $-OCH_3$  groups on the salicylidene rings. This group donates the electrons to the salicylidene rings by the mesomeric effect. The ligand  $H_2L^1$  has more positive anodic and cathodic data than the ligand  $H_2L^2$ . Furthermore, it can be deduced from the calculated  $E_{1/2}$  that these compounds cannot be easily oxidized nor can they be reduced. Thus, in order to use them successfully in redox reactions, some structure modifications to decrease the  $E_{1/2}$  would have been required. In a reversible redox process, the transferred charge in the reduction and in the oxidation stages is the same, and thus their ratio is unity. However, in compounds, at a scan rate of  $100\text{ mVs}^{-1}$ , this charge ratio is higher. This may be due to the fact that reduction takes place at a lower rate than oxidation and that some oxidized material may be adsorbed on the electrode's surface. On increasing the scan rate from 100 to  $500\text{ mVs}^{-1}$ , the reduction-oxidation waves become more

irreversible. Probably, this change is due to the increase in the scan rate and diffusion problems occur.

The ligands  $H_2L^1$  and  $H_2L^2$  showed mutagenic activity on the strain TA 100, with and without the S9 mix. In the absence of the S9 mix, the mutagenic activity of the ligand  $H_2L^2$  on the TA 100 strain or TA 98 was observed to be dose-dependent. According to data obtained from the Ames test, all tested ligands and their various metabolites induced the frameshift mutation (TA 98). In addition, the ligands  $H_2L^1$  and  $H_2L^2$  and also their metabolites induced the base-pair substitutions (TA 100).

## References

- [1] H. Schiff, *Ann. Chim (Paris)* **131**, 118 (1864).
- [2] S. Dayagi, Y. Degani, in: S. Patai (Ed.), *The Chemistry of the Carbon-Nitrogen Double Bonds*, 117, 1970.
- [3] M. Calligaris, L. Randaccio, in: G. Wilkinson (Ed.), *Comprehensive Coord. Chem.* **2**, 715 (1987).
- [4] F. P. Dwyer, D. P. Mellor, *Chelating Agents and Metal Chelates* (Acad. Press), 1964.
- [5] M. Tümer, *J. Coord. Chem.* **60**, 2051 (2007).
- [6] Rigaku/MS, CrystalClear. Rigaku/MS, The Woodlands, Texas, USA, 2005.
- [7] G. M. Sheldrick, (SHELXS-97) and (SHELXL-97), University of Gottingen, Germany, 1997.
- [8] A. Kayraldız, F. F. Kaya, S. Canımoğlu, E. Rencüzoğulları, *Annals of Microbiology.* **56**, 129 (2006).
- [9] M. Aslantaş, M. Tümer, E. Şahin, F. Tümer, *Acta Cryst.* **E63**, o644 (2007).
- [10] L. J. Farrugia, *J. Appl. Cryst.* **30**, 565 (1997).
- [11] M.-H. Yang, Y. -F. Zheng, G. -B. Yan, *Acta Cryst.* **E63**, o982 (2007).

\*Corresponding autor: ccelik@ksu.edu.tr